Measurement and Analysis of the Diameter of Appendix Based on Ultrasound Images

J. Lam, C. Pahl, H. N. Abduljabbar, and E. Supriyanto

***Abstract*—One of the most common cause of emergency surgery of the abdomen is acute appendicitis. Early and accurate diagnosis of appendicitis can decrease the morbidity and hospital cost by reducing the delay in diagnosis of appendicitis and its associated complications. In current clinical practice, the measurement of the outer appendiceal diameter by sonographers has been used as one of the indication to confirm acute appendicitis, where the value greater than 6 mm is considered to be a sign of acute appendicitis. However, since ultrasound image itself is in low quality due to speckle noise, error in manual measurement by the sonographers might occur due to wrong detection of the appendiceal edge or wrong placement of the calliper. Thus, we propose certain image processing techniques to enhance the image quality to help sonographers in performing a better diagnosis. This paper proposed a series of image processing method including image enhancement, image segmentation and edge detection before measuring the appendiceal. Selection of image enhancement method is made based on MSE and PSNR values while selection of image segmentation method is made based on the segmented image and execution time. Ten trials of measurement by sonographers using ultrasound and measurement after image processing were gathered. Statistical analyses of both measurements were computed. Mean and standard deviation for the sonographers measurements and measurements after image processing are 4.937±0.14mm and 4.613710±0.08mm respectively. Sonographers measurement showed higher variability compared to measurement after image processing thus measuring the appendiceal diameter after image processing can be helpful for a better diagnosis.**

***Index Terms*—Acute appendicitis, appendix ultrasound, edge detection, image enhancement, image segmentation**

I. Introduction

Appendix formally called vermiform appendix is a blinded-ended hollow tube structure that is attached at the end of the cecum [1], [2]. The appendix is located near the junction of small intestine and large intestine. The position of the appendix is different in each person as it is influenced by the change in position of the cecum, when it undergoes changes during development and growth [3] as in Fig. 1. Appendix arises from the cecum approximately 2.5cm below the ileocecal valve. Appendix varies in length in each human body [2]. The length of the appendix in infants or children is much longer compared to the adult body. This has been proven by scientists that the appendix is gradually disappearing in human body with time [1].

Manuscript received October 20, 2013; revised December 5, 2013.

Jostinah lam, Heamn N. Abduljabbar, and Eko Supriyanto are with Diagnostics Research Group, Universiti Teknologi Malaysia, 81310 Skudai Johor (e-mail: jostinah.lam@gmail.com; heamn_jabbari@yahoo.com; eko@utm.my).

Christina Pahl is with Diagnostics Research Group, Universiti Teknologi Malaysia, 81310 Skudai Johor and Ilmenau University of Technology in Germany (e- mail: pahl.christina@gmail.com).

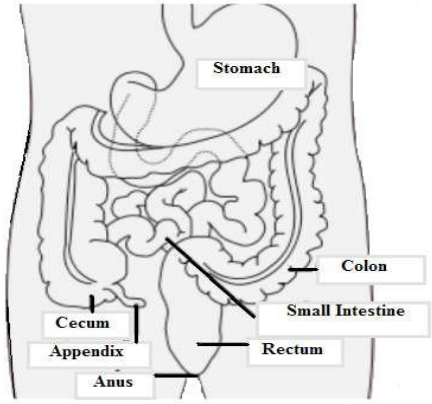

Fig. 1. Position of appendix in human body.

An acutely inflamed and enlarged appendix or known as the acute appendicitis is one of the most common surgical emergencies [4] worldwide and it requires prompt surgery to remove the appendix. People of any ages are exposed to this acute appendicitis problem and it is common in young adults and the most common surgical problem reported in children and pregnant women [5]. If one suffers from acute appendicitis, some complications can be seen including peritonitis, localized periappendicular abscess, thrombosis of portal vein drainage, liver abscess and septicemia [6] and the rate of these complications depends on the delay of diagnosis surgical treatment [7].

The outer appendiceal diameter is one of the most important established cross-sectional imaging criteria in the pre-operative evaluation of the appendix. According to the literature, the optimum cut-off point of the diameter measurement is still controversial [8]. The most common used cut-off point is 6 mm. A value greater than 6 mm is considered to be a sign of acute appendicitis, and a value less than 6 mm is regarded as typical for a normal appendix [9], [10].

Hence, accurate detection of the early sign of appendicitis is clinically important for prompt treatment. Medical imaging tools such as ultrasound, computed tomography (CT) scan, magnetic resonance imaging (MRI) [10], positron emission tomography (PET) and other diagnostic tools have been used to rule out or to confirm acute appendicitis [11]. Currently, diagnostic imaging nuclear medicine (NM) for appendicitis is not explored yet.

In present, computed tomography (CT) scan is the preferred tool compared to ultrasound and highly recommended when dealing with those patients who are obese, or have rigid non compressible abdomen, or may have complicated appendicitis such as rupture. However, for pregnant patient, the radiation exposure during diagnosis

using CT scan, doubled the risk to develop foetal abnormalities. This in turn makes ultrasound screening the more preferable method to examine appendicitis in pregnant patients.

Ultrasound imaging is widely used in clinical applicationsdue to its intuitive, convenient, safety, non-invasive, and low cost. Ultrasound with high resolution can be used to visualize the inflamed appendix and can be used to assess a variety of relevant disease [12]. The early and accurate diagnosis of appendicitis can decrease the morbidity and hospital cost by reducing the delay in diagnosis of appendicitis and its associated complications, as well as by avoiding in-patient observation prior to surgery in patient who presents with typical symptoms. Furthermore, ultrasound may provide alternative diagnosis which could be treated on outpatient basis [12].

The overall accuracy of ultrasound examination in thediagnosis of acute appendicitis in most of the studies was about 85%, so that it appears to be most useful in the early stage of the disease and it can be easily repeated to reach a final diagnosis [13]. The goal of radiologic imaging is to improve the number of true positive and decrease the number of false-negative and false positive that have confounded and mislead medical practices. In order to improve the accuracy of detecting acute appendicitis, an application of image processing method to the ultrasound images is suggested for better assessment of ultrasound image.

Many image processing methods are used to enhance ultrasound image in order to produce better and clearer image. The method was chosen based on the type of the image analysed and analysis to be made [14]. The image quality is affected by the noise occurred due to the acoustic nature of surrounding tissue. Hence, filtering techniques are required to remove the noise from the image. Based on previous study, MATLAB algorithm was created to enhance the ultrasound image quality by image segmentation and image enhancement methods [11]. The image was segmented using histogram thresholding and edge detection methods to enhance the quality of the image.

The paper is organized as follows. In Section II, we describe the proposed image processing method and implementation of outer appendiceal diameter measurement. Section III shows the result comparisons and analysis for manual appendiceal diameter measurement compared to ultrasound measurement. Finally, we summarize with discussions and conclusion.

II. Material and Methods

This section will discuss the overall methodology of this study. The study starts with data collection, image pre-processing and appendiceal diameter measurement. Lastly, statistical analysis was performed to analyze the data collected. Fig. 2 shows the overall process of the system performed in this study.

A. Data Collection

In this study, a total of ten trials of US examination of the vermiform appendix were performed. The appendix ultrasound images were taken using Aplio MX, Toshiba ultrasound machine available in the laboratory. The type of transducer implemented in current examination is the concave abdominal probe, with beam frequency of 3.5 MHz. The images were saved under DICOM format, both for the before and after manual measurement by sonographers. Fig. 3 shows the appendix image acquired in a coronal plane using ultrasound before the measurement of the appendiceal diameter and this image was used to be fed into image processing algorithm developed in this study. As can be seen in the Fig. 3, the appendix is not seen clearly through the ultrasound image.

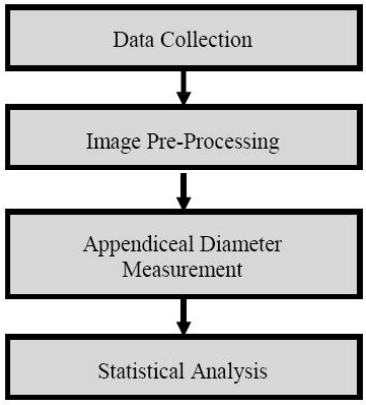

Fig. 2. Overall process of the system.

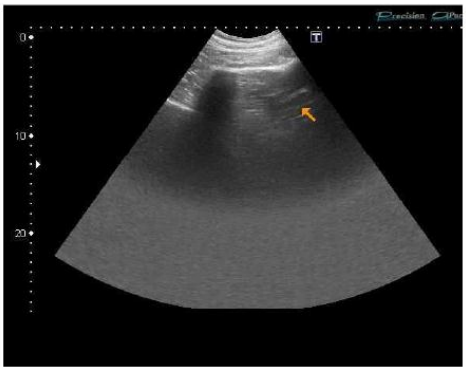

Fig. 3. Original appendix image.

B. Image Pre-Processing

In the proposed study, ultrasound images of the appendix collected underwent a series of image processing. Then the measurement of outer appendiceal diameter were made on the images processed using MATLAB. Fig. 4 illustrated the overall process implemented in this paper.

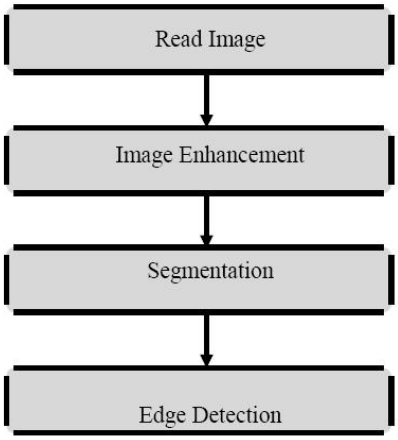

Fig. 4. Process flow chart.

First of all, appendix image in DICOM format was loaded to the MATLAB workspace. Then, the image was converted into grayscale image. This step was important for pre-processing of the image at later stage. In order to remove unwanted noise and enhance the image quality, the image enhancement method had been performed. After that, the image was segmented. This pre-processing method was to divide the image into its constituent region. The most suitable thresholding method was chosen to clearly segment the appendix in order to proceed to later works. Edge detection method was then implemented to detect sharp edges in the image, while preserving important structural properties of the image. Lastly, manual measurement of appendiceal diameter of the appendix was carried out.

1) Image enhancement

Image enhancement was used to improve the interpretability or perception of information in images for human viewers, or to provide optimal input for other automated image processing techniques. Many previous researches had compared different image enhancement techniques for ultrasound images [15]-[20]. In this study, four commonly used image enhancement techniques which have different fundamental theories had been applied on appendix ultrasound images. The techniques can be classified as nonlinear spatial domain filtering (median filter), frequency domain Gaussian low- pass filtering, histogram processing, and anistrophic diffusion (SRAD).

The assessment between the techniques applied was measured by the traditional distortion measurements such as MSE and PSNR between the original images and the output images. The mean-squared error (MSE) of the output image is defined as

$$MSE = \frac{\sum_{i=1}^{M}\sum_{j=1}^{N}|x(i,j)-\hat{x}(i,j)|^2}{MN} \quad (1)$$

where $x(i,j)$ is the original image, $\hat{x}(i,j)$ is the output image, and MN is the size of the image.

The peak signal-to-noise ratio (PSNR) is defined as

$$PSNR = \log_{10}[\frac{(2^n-1)}{\sqrt{MSE}}] \text{ [dB]} \quad (2)$$

where *n* is the number of bits used in representing the pixel of the image. For grayscale image, *n* is 8.

a) Nonlinear spatial domain filtering (median filter)

Median filter is designed by calculating the median value of the image [15]. In median filtering, the neighbouring pixels are ranked according to brightness (intensity) and the median value becomes the new value for the central pixel. This method sorted all the pixel values from the neighbourhood into numerical order and then replacing the pixel with the middle pixel value. It removes the noise of appendix image by reducing the speckle noise and hence improve the image quality [14].

b) Frequency domain gaussian low pass filtering

In frequency domain, the commonly used filter is the low-pass filter based on Gaussian function, since both the forward and the inverse Fourier transforms of a Gaussian are the real Gaussian functions. The transfer function of a Gaussian low- pass filter (GLPF) is given by

$$H(u,v) = e^{-D^2(u,v)/2\sigma^2} \quad (3)$$

where σ is the standard deviation and $D(u,v)$ is the distance from the origin of the Fourier transform [20].

c) Histogram equalization

Histogram equalization is an image processing used to improve the visual appearance of an image by adjusting the image histogram. Peaks in the image histogram (indicating commonly used grey levels) are widened, while the valleys are compressed [21].

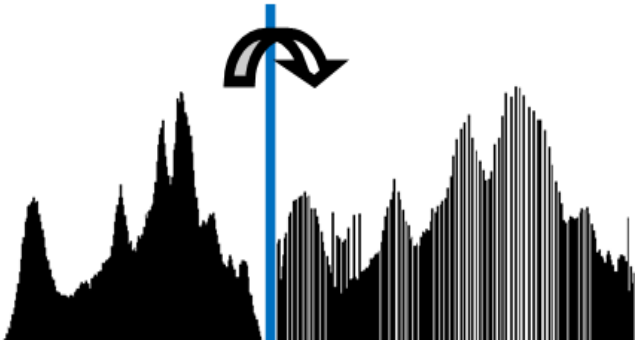

Fig. 5. Adjustment of a histogram to distribute intensities.

d) Anistrophic diffusion

Anistrophic diffusion speckle reduction (SRAD) proposed by Yu *et al*. is based on partial differential equation (PDE) which allows the generation of an image scale space without bias due to filter window size and shape. SRAD preserves and enhances edges by inhibiting diffusion across edges and allowing diffusion on either side of the edge. Besides, SRAD also does not utilize hard thresholds to alter performance in homogeneous regions or in regions near edges and small features [22].

Given an intensity image $I_0(x,y)$ having a finite power and no zero values over the image support Ω, the output image I(x,y;t) is evolved according to below PDE:

$$\begin{cases} \frac{\partial I(x,y;t)}{\partial t} = div[c(q)\nabla I(x,y;t)] \\ I(x,y;0) = I_0(x,y), (\frac{\partial I(x,y;t)}{\partial \vec{n}})|\partial\Omega = 0 \end{cases} \quad (4)$$

where $\partial\Omega$ denotes the border of Ω, $\vec{n}$ is the outer normal to the $\partial\Omega$, and

$$c(q) = \frac{1}{1+\frac{[q^2(x,y;t)-q_0^2(t)]}{[q_0^2(t)(1+q_0^2(t))]}} \quad (5)$$

or

$$c(q) = exp\left\{-\frac{[q^2(x,y;t)-q_0^2(t)]}{[q_0^2(t)(1+q_0^2(t))]}\right\} \quad (6)$$

where

$$q(x,y;t) = \frac{\sqrt{(\frac{1}{2})(\frac{|\nabla I|}{I})^2}}{[1+(\frac{1}{4})(\frac{\nabla^2 I}{I})]^2} \quad (7)$$

and $q_0(t)$ is the speckle scale function.

2) Image segmentation

To clearly analyse the image of appendix, the next step was to find out the suitable and most accurate method of

thresholding. The methods approached were Otsu's, Adaptive and proposed thresholding. All the images were analysed using each technique and the most clearly region of appendix's image was chosen and further continued to find out the area of the appendix.

a) Otsu thresholding

Otsu's thresholding method is an anatomically performing histogram-based image thresholding method. It implemented all the possible threshold values and measures all the pixel levels for each side of the threshold either foreground or background. The segmentation using Otsu's thresholding can be measured using variance value based on region homogeneity. In this method, it selects the threshold by minimizing the within-class variance (σ^2) or maximizing between class variance(σ^2), [23] given by (8) which reduced to as (9) which the term defines in (10) where n represents the number of grey levels and N is the total number of pixel in the image.

$$\sigma^2(t) = w_0(t)w_1(t)[\mu_1(t) - \mu_2(t)]^2 \quad (8)$$

$$\sigma^2(t) = w_0(t)[1 - w_0(t)[\tfrac{\mu - \mu_1(t)}{1 - w_0(t)} - \tfrac{\mu(t)}{w_0(t)}]] \quad (9)$$

$$w_0(t) = \textstyle\sum_N^n w_1(t) = 1 - w_0(t), \mu(t) = \sum t \tfrac{n}{N} \quad (10)$$

b) Adaptive thresholding

When a different thresholding is use for different regions in the image, it is so-called adaptive thresholding. It also known as local or dynamic thresholding [24]. Adaptive thresholding basically takes a grayscale or color image as input while outputs a binary image representing the segmentation. For each pixel in the image, a threshold has to be calculated. If the pixel value is below the threshold, it is set to the background value; otherwise it assumes the foreground value. It means that, if the average is lower than the average then it is set to black; otherwise it is set to white. This method compares a pixel to the average of nearby pixels, which will preserve hard contrast lines and ignore soft gradient changes.

c) Proposed thresholding

The proposed method defines the threshold level by multiplying the maximum gray level of the image with the normalized threshold value. This value is within the range of 0 to 1. The comparisons of thresholding image results with various normalized value is shown in Fig. 6. Comparing to the results seen in this figure the normalized threshold value of 0.009 is chosen for the discussed work.

d) Edge detection

The process of identifying the sharp discontinuities in an image is known as edge detection [23]. Canny edge detector is mainly refered to the gathering of the pixel that have strong changes and contain the useful information of identifying [24].Canny edge detection method is a modification of Sobel method [15].

In Canny, it detected the edges by inspecting the vertical and horizontal pixel intensity [23].This method searches the edge direction by implementing non-maximum suppression to sharpen the edge. To reduce the effect of the noise during edge detection, Canny also implemented Gaussian in its method. Compared to the other methods, Canny method provide good edge detection because of its good performance n term of single response to edge.

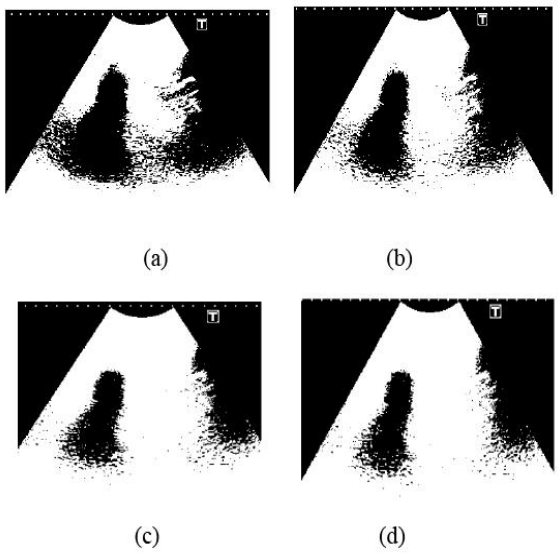

Fig. 6. Comparison of thresholded image results by proposed method with normalized threshold values: (a) 0.009, (b) 0.05, (c) 0.1 and (d) 0.4.

C. Appendiceal Diameter Measurement

The measured parameter was the outer appendiceal diameter using conventional 2D B-mode prenatal ultrasound scan protocol. In this study, the outer appendiceal diameters were measured perpendicularly as the distance between the outer borders of the hypoechoic tunica muscular (outer muscle coat) [25]. The ultrasound measurements were performed by the sonographer during US examination by setting the electronic callipers. For appendiceal measurements of processed image, measurements were made on processed appendix images by using MATLAB algorithm. Data obtained were then tabulated.

D. Statistical Analysis

Statistical analyses were performed using the SPSS 16 software (IBM SPSS Statistics). For the description of outer appendiceal diameters, baseline characteristics are presented as range, mean and standard deviation. The ultrasound and manual measurements of outer appendiceal diameter were compared in relations of standard mean error and variability.

III. Result and Analysis

This section will review and discuss on the result of each stage of image enhancement and image segmentation together with its appendiceal measurement and statistical analysis for validation purpose. The results were separated into image enhancement result, image segmentation result, edge detection and diameter measurement as well as statistical analysis result.

A. Image Enhancement Result

Firstly, image enhancement techniques were applied to all images. The techniques include nonlinear spatial domain filtering (median filter), frequency domain Gaussian low pass filtering, histogram equalization and SRAD. Table I shows the result of MSE and PSNR of different techniques while Fig. 7(a), Fig. 7(b), Fig. 7(c), and Fig. 7(d) show the result of the image enhancement techniques using median

filter, Gaussian low pass filter, histogram equalization and SRAD respectively. The results of the image enhancement is presented in Table I, with non linear spatial domain filtering having the MSE value of 0.007 and PSNR(dB) of 45.63, frequency domain Gaussian low-pass filtering having MSE value of 0.018 and PSNR(dB) of 41.57, histogram equalization having the MSE value 0.225 and PSNR (dB) 30.55 and SRAD having the MSE value of 0.017 and PSNR (dB) 41.63. Based on the result, median filter is chosen to be performed for this study purpose, due to it having the lowest MSE and highest PSNR (dB).

TABLE I: MSE AND PSNR OF DIFFERENT IMAGE ENHANCEMENT TECHNIQUES

Enhancement Techniques	MSE	PNSR (dB)
Nonlinear Spatial Domain Filtering (Median Filter)	0.007	45.63
Frequency Domain Gaussian Low-pass Filtering	0.018	41.57
Histogram Equalization	0.225	30.55
Speckle Reduction Anistrophic Diffusion (SRAD)	0.017	41.63

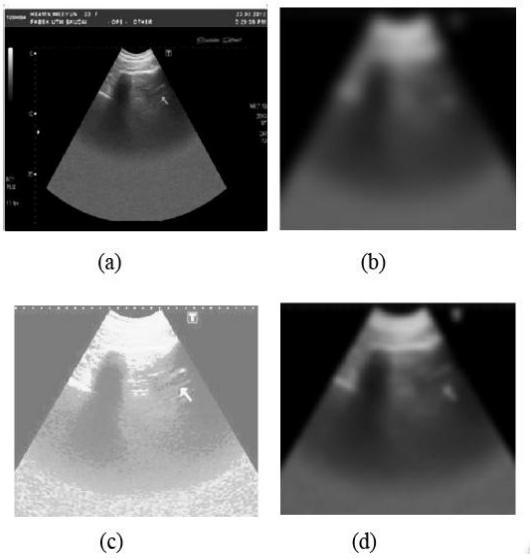

Fig. 7. Image enhancement technique using, (a) median filter, (b) Gaussian low pass filter, (c) histogram equalization, (d) SRAD.

B. Image Segmentation Result

In order to find out the proper and most suitable method for appendix segmentation, we analyzed all the thresholding techniques. Table II shows the resultant appendix images with different thresholding method and its execution time. From Table II, we can see that the Otsu Thresholding has an execution time of 0.225s, adaptive thresholding 76.827s and proposed method 0.244s. Both images produced from adaptive and proposed thresholding methods showed better quality of visualization compared to Otsu's method. However, the execution time for adaptive method was much longer compared to the others two methods. Hence, proposed thresholding method was suggested as the most proper method to segment out the appendix for appendiceal diameter measurement.

C. Edge Detection and Diameter Measurement

Canny edge detector is an edge detection operator that uses a multi-stage algorithm to detect a wide range of edges in images. Hence, Canny edge detector was performed for edge enhancement to identify edges which then become candidates for boundaries of the image. The resulting image is displayed in Fig. 8.

TABLE II: COMPARISON OF THRESHOLDING METHODS FOR APPENDIX SEGMENTATION

Segmentation Method	**Result**	**Time (s)**
Otsu Thresholding	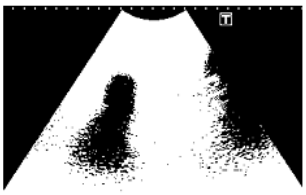	0.225
Adaptive Thresholding	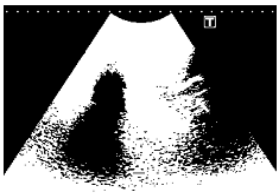	76.827
Proposed Thresholding	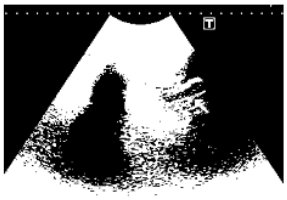	0.244

Fig. 8. Appendix image after Canny edge detection.

From the results, it can be seen that the implemented image processing clearly outline the appendix. This makes the evaluation easier by measuring the distance of the appendiceal diameter. However the whole appendix cannot be detected. Some region of the appendix had been cut off due to the discontinuity of the pixel in the image after edge detection. This may be due to the poor image quality captured by the ultrasound and inappropriate use of probes when examining which in turn give a low quality and blurry image.

These factors highly affect the quality of the image.

After a series of image processing, appendix can be visualized clearly and measurement can be made easily by MATLAB algorithm. The outer appendiceal diameters were measured perpendicularly to the long axis as shown in Fig. 9. The measurements were then tabulated.

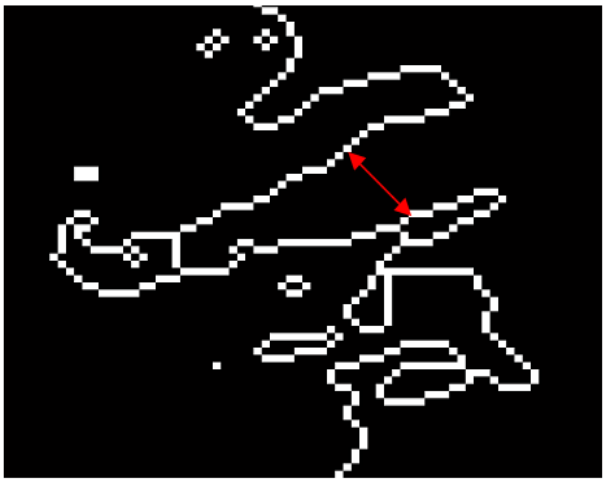

Fig. 9. Outer appendiceal diameter measurement.

TABLE III: SUMMARY OF SONOGRAPHERS MEASUREMENT AND MEASUREMENTS AFTER IMAGE PROCESSING OF APPENDICEAL DIAMETER

No of Trial	Appendiceal diameter (mm)	
	Measurement by sonographer	Mesurement using Matlab
1	4.81	4.70
2	4.79	4.50
3	4.98	4.53
4	5.13	4.70
5	4.85	4.70
6	4.77	4.53
7	5.07	4.65
8	4.93	4.61
9	4.88	4.53
10	5.16	4.70

TABLE IV: SUMMARY OF STATISTICAL ANALYSIS OF ULTRASOUND AND MANUAL APPENDICEAL DIAMETER MEASUREMENTS IN MM

Type of Measurement	N	Min	Max	Mean		Std. Deviation
	Statistic	Statistic	Statistic	Statistic	Std.Error	Statistic
Measurement by sonographer	10	4.770	5.160	4.937	0.045	0.143
Measurement using MATLAB	10	4.501	4.704	4.614	0.027	0.084

D. Statistical Analysis

Measurement of outer appendiceal diameter was conducted using MATLAB. The results were compared to the ultrasound measurement made by sonographer during ultrasonography appendix examination. The data were then tabulated and analysed. From Table III, the range of the deviation from measurements by sonoraphers were much larger compared to measurement after image processing, varying from minimum values 4.77mm to maximum values 5.16mm. Statistical analyses of sonographers measurements and measurement after image processing were computed Table IV shows the difference of their means and standard deviations. As indicated in Table IV above, the computed mean and standard deviation for sonographers measurements are much larger compared to measurement after image processing, which are 4.937 ± 0.1425989mm and 4.613710 ± 0839246mm respectively. This revealed that sonographers measurement had higher variability than measurement after image processing. In comparison of standard error, sonographers measurement (0.0450937mm) shows greater value compared to measurement after image processing (0.0265393mm). The comparison results showed a higher consistency of the measurement after image processing compared to sonographers measurement. This may be due to low quality image acquired during appendix examination. This in turn induced human error which affects the placement of calliper by sonographer during appendiceal diameter measurement.

IV. CONCLUSION

Accurate appendiceal diameter measurement is essential for appendicitis early detection. It is feasible to perform a much safer appendix examination to all range of patient using ultrasound. In our study, a new approach on ultrasound appendiceal diameter measurement has been developed. This project perform few image enhancement method consist of medial filter, Gaussian low pass filter, histogram equalization and SRAD. Measurement of MSE and PSNR of output images show that median filter give better result with MSE of 0.007 and PSNR of 45.63dB. Few image segmentation techniques were also compared and we proposed new thresholding technique that can segment the appendix better, with relatively short execution time. This helped in diameter measurement at later stage where the outline of appendix were more clearly defined after image processing. It can be observed that the proposed measurement after image processing had greater advantages compared to sonographers measurement, in terms of its visualization and measurement consistency. Further research is necessary to standardize the image scanning angle and probe view to minimize artifacts in producing uniform images.

ACKNOWLEDGMENT

The authors of this paper would like to thank the subjects consented for data collection, Universiti Teknologi Malaysia and Biotechnology Research Alliance for the required facilities, and Ministry of Higher Education (MOHE) Malaysia for supplying the grant Vot No. Q.J130000.2536.02H96. for the implementation of projects.

REFERENCES

[1] Appendix. Encyclopædia Britannica. [Online]. Available: http://global.britannica.com/EBchecked/topic/30542/appendix

[2] H. F. Smith *et al.*, "Comparative anatomy and phylogenetic distribution of the mammalian cecal appendix," *Journal of Evolutionary Biology*, vol. 22, no. 10, pp. 1984-1999, 2009.
[3] R. J. Berry, "The true caecal apex, or the vermiform appendix: Its minute and comparative anatomy," *Journal of Anatomy and Physiology*, vol. 35, no. 1, pp. 83-100, 1900.
[4] Puylaert, "Acute appendicitis. Ultrasound evaluation using graded compression," *Radiology*, vol. 158, no. 355, 1996.
[5] S. L. Robbins and R. S. Cotran, "The gastrointestinal tract in pathologic basis of disease," *Philadelphia WB Saunders*, vol. 918, 1997.
[6] H. C. Yeh and J. G. Rabinowitz, "Ultasonography of gastro intestinal tract," *Semin Ultrasound CT MR*, vol. 3, no. 331, 1982.
[7] M. C. Horattas, D. P. Guyton, and D. Wu "A reappraisal of appendicitis in elderly," *Am. J Surgery*, 1990; vol. 160, pp. 291-293, 1990.
[8] H. V. Nghiem and R. B. Jeffrey Jr., "Acute appendicitis confined to the appendiceal tip: evaluation with graded compression sonography," *J. Ultrasound Med.*, vol. 11, no. 5, pp. 205-207, 1992.
[9] R. B. Jeffrey, Jr., F. C. Laing, and R. R. Townsend, "Acute appendicitis: sonographic criteria based on 250 cases," *Radiology*, vol. 167, no. 2, pp. 327-329, 1988.
[10] G. M. Israel *et al.*, "MRI vs. ultrasound for suspected appendicitis during pregnancy," *Journal of Magnetic Resonance Imaging*, vol. 28, no. 2, pp.428-433, 2008.
[11] E. Supriyanto, M. Wider, and Y. M. Myint, "Ultrasound appendix image segmentation using histogram thresholding and image enhancement using noise filtering technique," in *Proc. the 15th WSEAS International Conference on Computers*, World Scientific and Engineering Academy and Society (WSEAS): Corfu Island, Greece, 2011, pp. 223-227.
[12] H. K. AL-Allaf, "Validity of ultrasound examination in the diagnosis of acute appendicitis compared with surgical results," *Annals of the College of Medicine*, vol. 33, no. 1&2, 2007.
[13] M. M. W. Fortscher, "Ultrasound first in acute appendix? Unnecessary laparotomies can often be avoided," *Med.* vol. 142, pp. 29-32, 2000.
[14] E. Supriyanto *et al.*, "Segmentation of prostate tumor for gamma image using region growing method," in *Proceedings of the 15th WSEAS International Conference on Computers*, World Scientific and Engineering Academy and Society (WSEAS): Corfu Island, Greece. pp. 189-194, 2011.
[15] W. M. Hafizah, W. W. Yun, and E. Supriyanto, "Optimization of pancreas measurement techniques based on ultrasound images," *WSEAS Transactions on Biology and Biomedicine*, vol. 8, no. 4, pp. 135-144, 2011.
[16] H. Y. Chai, L. K. Wee, and E. Supriyanto, "Ultrasound images edge detection using anisotropic diffusion in canny edge detector framework," *WSEAS Transactions on Biology and Biomedicine*, vol. 8, no. 2, pp. 51-60, April 2011.
[17] Z. Ke, Y. J. Sha, and Y. X. Ming, "Edge detection of images based on cloud model cellular automata," *WSEAS Transactions on Biology and Biomedicine*, vol. 4, no. 5, pp. 67-72, May 2007.
[18] J. Canny, "A computational approach to edge detection," *IEEE Trans. Pattern Anal. Mach. Intell.*, vol. 8, no. 6, pp. 679-698, 1986.
[19] T. Rettenbacher *et al.*, "Outer diameter of the vermiform appendix as a sign of acute appendicitis: Evaluation at US1," *Radiology*, vol. 218, no.3, pp. 757-762, 2001.
[20] W. M. Hafizah and E. Supriyanto, "Comparative evaluation of ultrasound kidney image enhancement techniques," *International Journal of Computer Applications*, vol. 21, no. 7, pp.15-19, 2011.
[21] H. D. Cheng and X. J. Shi, "A simple and effective histogram equalization approach to image enhancement," *Digital Signal Processing*, vol. 14, pp. 158–170, 2004.
[22] Y. Yu and S.T. Acton, "Speckle reducing anistrophic diffusion," *IEEE Trans* on *Image Process*, vol. 11, pp. 1260-1270, 2002.
[23] H. Tian, S. K. Lam, and T. Srikanthan. "Implementing Otsu's thresholding process using area-time efficient logarithmic approximation unit," in *Proc. the 2003 International Symposium on Circuits and Systems*, 2003.
[24] F. Abramovich and Y. Benjamini, "Adaptive thresholding of wavelet coefficients," *Computational Statistics & Data Analysis*, vol. 22, no. 4, pp. 351-361, 1996.
[25] W. M. Hafizah and E. Supriyanto, "Automatic region of interest generation for kidney ultrasound images," in *Proc. the 11th WSEAS International Conference on Applied Computer Science*. *2011*, World Scientific and Engineering Academy and Society (WSEAS): Penang, Malaysia. 2011, pp. 70-75.

Jostinah Lam was born in Sabah, Malaysia. In 2011, she graduated from University of Technology Malaysia in Biomedical Engineering. She is currently pursuing her double degree master in Biomedical Engineering from UTM and University of Technology Ilmenau, Germany. Her research interests are medical imaging, medical informatics, semantic web and medical image processing.

Heamn Noori Abdul Jabbar is a medical sonographer of IJN-UTM Cardiovascular Engineering Centre. He has 8 years of experience in medical ultrasound scanning. He obtained his Bachelor of Radiology from Baghdad University Iraq. He has a Master in Biomedical Engineering from UTM. He has more than 7 international publications. His research interests are fetal echocardiography, general ultrasound, and biomedical imaging.

Eko Supriyanto is born in Demak, Indonesia. He graduated from Bandung Institute of Technology in Biomedical Engineering. He obtained his PhD from University of Federal Armed Forces Hamburg Germany. He is currently a full professor and director of IJN- UTM Cardiovascular Engineering Centre. He has more than 130 publications and 30 international awards. His research interests are medical imaging, medical informatics, electronics, biomaterials and biotechnology.